Acta Protozool. (2023) 62: 45–56
www.ejournals.eu/Acta-Protozoologica
doi: 10.4467/16890027AP.23.005.18868

ACTA
PROTOZOOLOGICA

The function of ciliopathy protein FOP on cilia and cortical microtubule cytoskeleton in *Euplotes amieti*

Junlin WU*, Jiaqi YIN*, Zixiang XU, Yingli LIU, Huanyong QIN, Xin SHENG

Department of Biochemistry, Zunyi Medical University, Zunyi, Guizhou, China

*** These authors contributed equally to this work.**

Abstract. FOP is a centriole satellite protein involved in ciliogenesis. Although centriole satellites are involved in centrosome and cilium-related protein trafficking, their functions related to ciliary assembly and maintenance of ciliary microtubule stability remain unclear. In this study, the function of the *FOP* gene in *Euplotes amieti* was investigated by interfering with its expression using RNAi. As a result, expression levels of the ciliary assembly-related proteins BBS8 and IFT88 were down-regulated. Swimming speeds also decreased and the Euplotes were only able to spin in circles, which suggested that the FOP protein is an important protein involved in ciliary motion. Further observations of *Euplotes amieti* microstructure and ultrastructure via immunofluorescence and transmission electron microscopy revealed that FOP not only participated in the formation of the ventral ciliary basal body but also played an important role in the maintenance of cortical microtubules, which is fundamental for the morphological structure of *Euplotes amieti*.

Keywords: *Euplotes amieti*, FOP, cortical microtubule, cytoskeleton, cilia

INTRODUCTION

Cilia are organelles widely distributed from protozoa through to humans and exist on the surface of most cells (Goetz and Anderson 2010). They play important roles in the development of the organism and the maintenance of normal physiological functions of tissues and organs. Cilia are highly evolutionarily conserved. They are composed of a basal body, transition zone, axoneme, ciliary membrane, and ciliary tip (Dentler 1980). The basal body is a compact particle in the root of the cilium, with a diameter of about 200 nm measuring around 550 nm long. The basal body is homologous to centrosomes, and its core structure is evolutionarily conserved. It is a hollow structure enclosed by nine triplet microtubules and can be roughly divided into three parts: proximal, basal cavity, and distal, based on its ultrastructure (Pearson and Winey 2009; Bayless et al. 2015). As an important structure of cilium, the basal body is the basis of cilium assembly and is also involved in the initiation and anchoring of non-cilium microtubule assembly. However, much key information about the protein composition of basal bodies and their specific functions remains elusive. Most ciliary proteins are evolutionarily conserved and play the same

Address for correspondence: Xin SHENG, Department of Biochemistry, Zunyi Medical University, Zunyi, Guizhou 563003, China; Email: xshengbio@163.com; Tel.: +86 18212136401; Fax: +86 21 6408 5875

role within the motile cilia of protozoa and vertebrates, including humans. Due to these similarities, protozoa became an attractive biological model for studying ciliary biology in general. Recent studies using protozoa, particularly ciliates, have shown that some of the core modules of multicellular signaling pathways are present and are preserved in unicellular organisms. Furthermore, ciliates have distinct tubulin gene isoforms and, therefore, may help unravel the changes in microtubule stability found in metazoan cells, including humans (Libusová and Dráber 2006).

In recent years, some studies have demonstrated that the basal body is involved in microtubule modification which can maintain microtubule stability. Loktev et al. (2008) found that knocking out the human retinal pigment epithelium ciliary basal body protein BBIP10 inhibited ciliary assembly by reducing intracellular tubulin acetylation levels. In contrast, Berbari et al. (2013) established that loss of cilia resulted in excessive acetylation of tubulin. In Tetrahymena, the basal body protein Poc1 maintained basal body stability by increasing the connections between the triplet microtubules (Meehl et al. 2016). Therefore, starting from the basal body and its associated proteins, we can explore the molecular regulation mechanism governing the assembly of ciliary and cortical microtubule cytoskeletons in ciliates.

Proteomic studies of cilia have revealed that there are more than 1,000 proteins involved in ciliary structure, function, and assembly (Gherman et al. 2006). Mutations in more than a thousand ciliopathy-related proteins, spanning the tubulin, centrosome, Bardet-Biedl syndrome (BBS), and intraflagellar transport (IFT) family proteins, are known to contribute to various ciliopathies, such as polydactyly, polycystic kidney disease, infertility, and other related conditions (Chen et al. 2023). These proteins are called ciliopathy-associated proteins. At present, 187 ciliopathy-associated proteins and 241 candidate proteins have been found (Reiter and Leroux 2017). Most of these were found to be localized in the basal body. For example, the BBS family proteins (Forsythe et al. 2018), which are predominantly localized to basal body, are involved in the transport of Golgi apparatus vesicles during ciliary assembly and ciliogenesis (Mockel et al. 2011). Nephronophthisis (NPHP), Marfan Syndrome (MKS), and the IFT protein families are also localized in the distal transition zone of basal body (Williams et al. 2011; Deane et al. 2001). Recently, it was shown that alterations in the *FOP* gene, lead to Crohn's disease, Graves's disease, and vitiligo (Cabaud et al. 2018; Shen et al. 2016). FOP was initially found in patients with a rare stem-cell myeloproliferative disorder (Vizmanos et al. 2004). It is a fusion partner of FGFR1, also known as the FGFR1OP. FOP is an important component of the centrosomal satellite and was shown to be involved in cilium formation (Mikolajka et al. 2006). Although centrosomal satellites are implicated in the transportation of proteins associated with centrosomes and cilia, the roles of FOP in ciliate basal body localization, cilium assembly, depolymerization, and microtubule morphogenesis remain unclear.

To assess the cellular and subcellular localization of FOP, immunofluorescence, and transmission electron microscopy techniques were used. FOP was mainly localized in the nucleus, and basal body of ventral ciliary organs (adoral zone of membranelles, caudal cirrus, frontal ventral cirrus, transverse cirrus), and their accessory microtubules. The role of FOP in ciliary dynamics, ciliary assembly, and stability maintenance of cortical microtubule cytoskeleton was explored by silencing its gene using RNAi. These results provided information vital for further exploration of the mechanisms of regulation and maintenance of the assembly and stability of cortical microtubule cytoskeleton in hypotrichous ciliate.

MATERIALS AND METHODS

Cultural conditions of *Euplotes amieti* and *Clostridium elongatum*

Euplotes amieti was obtained from a farm pond near the Qingpu District, Shanghai. The Euplotes were cultured in the laboratory and purified. The water temperature was 25 ± 0.5 °C, and the *Euplotes amieti* were fed on *Clostridium elongatum*. To avoid the interference of chlorophyll in green algae, 500–1000 mL *Clostridium elongatum* was fed to cells in each 500 mL suspension, and the feeding was stopped after the cells reached the logarithmic growth period. *Euplotes amieti* fed with green algae were transferred to 50 mL of pure water for 72 hours and the experiment was then performed.

The *Clostridium elongatum* was cultured in Synthetic Medium for Chlorogoium (SMC) in a 25 °C constant temperature illumination incubator. When the green algae turned yellow, it was recultured in an agarose solid culture medium, the clones were selected and inoculated into the SMC medium.

Construction of interference expression vector

The total genomic DNA of *Euplotes amieti* was extracted, and the *FOP* gene was amplified and ligated with the pMD18-T vector (Primers are in Table 1). The target band was then ligated using the L4440 vector after double digestion with restriction enzymes (*Hind* III

Table 1. Primers used for FOP gene amplification.

Gene	Primer sequence (5′ to 3′)	Product length (bp)
FOP	F: TCCGATCTCCCCAAAACCCC	1162
	R: TTCCGATCTCCCCAAAACCCC	

and *Sma* I) and transformed into RNaseIII-deficient in *E. coli* HT115. The plasmid was extracted from the transformed positive clone strain and sequenced (Sangon Biotech, Shanghai, China). The sequence alignment of the recombinant plasmid L4440-FOP was completely identical to the genomic *FOP* gene in the support information.

Bacteria were divided into two groups: the gene silence group is the *E. coli* HT115 containing the recombinant expression vector L4440-FOP, and the blank group is the *E. coli* HT115 containing an empty plasmid vector L4440 which did not have the *FOP* gene fragment inserted. Both groups of bacteria were fed separately to *Euplotes amieti* following the method reported by Paschka et al. (2003).

For RNAi, 100 mL dilution of cultured *E. coli* HT115 was inoculated into LB liquid medium and cultured at 210 rpm and 37 °C for 180 min. When OD_{600} = 0.4, IPTG was added to achieve a final concentration of 0.4 mM and was then cultured for 4 hours to induce the expression of dsRNA. The bacteria were eluted with 1 mL of double-distilled water and fed with 30 μL of dsRNA-expressing *E. coli* HT115 every 2×10^6 euplotes.

Immunofluorescence

The cells were fixed in 4 % paraformaldehyde at room temperature for 10 min and transferred onto poly-L-lysine coated slides, permeabilized with 0.5 % TritionX-100. Cells were blocked in 0.1 M PBS with tween (PBST) containing 3 % bovine serum albumin (BSA) for 30 min at room temperature and incubated in a rabbit anti-human FOP polyclonal primary antibody (1:1600) (Proteintech, Cat No. 11343-1-AP, China) overnight at 4 °C. After washing, cells were incubated in the coralite488-conjugated goat anti-rabbit IgG (H+L) (1:200) (Proteintech, Cat No. SA00013-2, China) for 45 min at room temperature. Cells were briefly washed and covered with 15 μL Slowfade Gold Antifade Mountant with DAPI (Thermo Fisher Scientific, USA). Images were then acquired with an Olympus IX81 (Japan) fluorescence microscope. For Flutax-2 staining, cells were fixed and then incubated in Flutax-2 (Oregon Green™ 488 conjugate, Invitrogen, USA) for 10 min at RT without permeabilization.

Immunoelectron microscopy

The cells were fixed in a fixative solution containing 2 % paraformaldehyde and 0.25 % glutaraldehyde (1:1) for 60 min, and dehydrated in gradient acetone dehydration (30 %, 50 %, 60 %, 70 %, 80 %, 90 %, and 100 %) for 15 min each. Then, cells were gradually permeated in a 1:1 and 1:3 mixture of LR-White embedment and 100 % ethanol for 60 min, and in pure LR-White embedment overnight. LR-White pure entrapment agent was applied on a shaking bed for 2 hours. Finally, cells were embedded in a pure LR-White embedment at 50 °C for 48 h. The blocks were cut into 50 nm sections and treated with 1 % H_2O_2 for 15 min to repair the antigens and then blocked with 0.1 M PBS containing 3% BSA for 60 min. Cells were incubated in a rabbit anti-human FOP polyclonal primary antibody (1:1000) (Proteintech, Cat No. 11343-1-AP, China) at room temperature for 2 hours, then in the 10 nm colloidal gold-conjugated goat anti-rabbit IgG (1:20) (Sigma-Aldrich, Cat No. G3779, USA) for 1 hour at room temperature. Finally, samples were stained with 2 % uranyl acetate for 60 min and visualized using a transmission microscope (JEM-1400).

Western Blotting

Cells were harvested and lysed in cell lysates containing 1 % protease inhibitors (Merck, USA) for western blotting to detect protein expression. Protein concentration was determined using a BCA kit (Merck, USA). Then 20 μg of each protein sample was separated in an 8 % polyacrylamide gel and transferred onto polyvinylidene difluoride membranes in electro-blotting buffer (0.58 % Tris base, 0.29 % glycine, 0.037 % SDS, 1 % methanol) at 4°C for 120 min. Subsequently, the membranes were blocked in TBST buffer with 1 % skimmed milk for 2 hours at RT and respectively incubated with rabbit anti-human FOP (1:2000, Proteintech, China), rabbit anti-human β-tubulin (1:10000, Abcam, USA), rabbit anti-human BBS8 (1:500, Proteintech, China), rabbit anti-human IFT88 (1:1500, Proteintech, China), mouse anti-human γ-tubulin (1:10000, Sigma-Aldrich, USA), rabbit anti-human β-actin (1:10000, Proteintech, China) overnight at 4 °C, followed by peroxidase-conjugated sheep anti-rabbit/mouse IgG secondary antibody (1:2000, Thermo Fisher Scientific, USA) for 2 hours at RT, respectively. Finally, the membranes were quantified by enhanced chemiluminescence (ECL) reagents (Clarity™ Western ECL Substrate; Bio-Rad Laboratories, Inc., Hercules, CA, USA) and quantified using Quantity One software 4.6.7 (Bio-Rad Laboratories. Inc., USA). The ratio of the optical density of the target protein to the optical density of β-tubulin or β-actin was estimated as the relative expression level of the target protein.

Swimming speed and trace determination

4–8 *Euplotes amieti* cells were transferred onto Petri dishes (90 mm in diameter), covered with slides, and photographed every 0.3 sec under a 10 × microscope objective. The swimming trace was analyzed using Image J, and the swimming speed was analyzed using Prism.

Statistical analysis

All experiments were repeated three times. All data are presented as the means ± standard error of the mean. Two independent samples t-tests were used for comparative analysis between the two groups and data were statistically analyzed using GraphPad Prism. $P < 0.05$ was considered statistically significant.

RESULTS

FOP was localized to the microtubule organelles of the ventral cilia and the macronucleus of *Euplotes amieti*

Ciliates are protozoa covered with cilia on their cell surface. *Euplotes* are typical hypotrichous ciliate. It contains an extremely complex cortical microtubular

cytoskeleton and various types of microtubule-organizing centers. The cilia are highly differentiated into motile ventral cilia and non-motile dorsal kineties. The cilium is continuously depolymerized and reorganized within the cell cycle (Ishikawa and Marshall 2011; Bouhouche et al. 2022), which is regulated by several centriole proteins. In *Euplotes amieti*, the ventral ciliary organelles are formed by the adoral zone of membranelles (AZMs), one paroral membrane (Pm), nine frontal–ventral cirri (FVCs), five transverse cirri (TCs), two caudal cirri (CCs), and two left marginal cirri (LMCs). There are also several ciliary-associated microtubules in the ventral cortex, such as the anterior longitudinal microtubules (ALM) and posterior longitudinal microtubules (PLM) (Fig. 1A). To determine whether FOP is localized at the basal bodies in *Euplotes amieti,* FOP was labeled using an immunofluorescence technique, and its localization in *Euplotes amieti* was observed using fluorescence microscopy.

The immunofluorescence results showed that the macronucleus of *Euplotes amieti* was a digital "3" type, as noted via DAPI staining (S1A). FOP was mainly localized at the base of the ventral ciliary organelles, including the AZM, Pm, FVC, TC, CC, LMC, and their accessory microtubules, including ALM and PLM (Fig. 1B and C). As a centriole protein, FOP is an important protein for cilium formation (Lee and Stearns 2013). However, it was not observed on the dargyrome or at the base of the dorsal kineties. To further clarify the localization of FOP in *Euplotes amieti*, the subcellular localization of FOP was observed by immunoelectron microscopy. These investigations showed that, in *Euplotes amieti*, FOP was localized at the basal bodies and their surrounding microtubules, the ridge between transverse cirrus, and the macronucleus (Fig. 1D, S1B).

Taken together, these findings indicate that FOP is predominantly localized in the basal bodies of the ventral cilia and the ciliary associated microtubules in *Euplotes amieti*.

Silencing of FOP was lethal for *Euplotes amieti*

We performed RNAi by feeding *E. coli* HT115 containing recombinant plasmid L4440-FOP dsRNA. Cells were divided into three groups: the normal group was fed with *C. longiflorum*, the blank group was fed with *E. coli* HT115 containing an empty plasmid vector, and the RNAi group was fed with *E. coli* HT115 containing a recombinant plasmid expressing FOP dsRNA. The growth curves showed that the number of *Euplotes amieti* in the normal and blank groups gradually increased from days 2–6, but population decline in the blank group was observed from day 6, possibly because *E. coli* could not provide the nutrients needed for ciliate growth. However, the number of *Euplotes amieti* in the interference group decreased from day 2, and by day 10 the entire population had died (Fig. 1F). The cell sizes were also compared between the normal group and the RNAi group, the length of the cell becomes smaller after interference, but there are no differences between the RNAi groups (S2E). On the 9th day, the wide of the cells were smaller than the normal cells (S2F). As a result, the cell aspect ratio on the 9th day was also bigger than that on the 7th day (S2G). In conclusion, following FOP expression interference, *Euplotes amieti* growth was inhibited, and silencing of FOP was lethal for *Euplotes amieti*. Due to these effects, the Euplotes following 9 days of feeding with the interfering plasmid were used for the follow-up experiment. To confirm the expression level of FOP after RNAi, we detected them by qPCR and western blotting, the results showed that the expression of FOP was significantly downregulated in the interference group than that in the blank group, however, there were no significant differences between the normal and blank group expression levels (Fig. 1G and H). These results indicate that the gene silencing of FOP was successful by interfering FOP by feeding.

Following these observations, an anti-FOP antibody was used to detect the localization of the FOP protein

➤➤

Figure 1. Expression and localization of FOP before and after RNAi in *Euplotes amieti.* (A) The pattern diagram of basal bodies of ventral cirri and their accessory microtubules in *Euplotes amieti*. (B, C) Localization of FOP in the ventral cortex, arrows indicate the ciliary-associated microtubules, such as the PLM and ALM, bar = 20 μm. (D) Immuno-electron microscopy view of FOP, which is localized at the basal bodies of ventral cilia, arrows indicate the gold particles, for the above figure, bar = 1 μm, for the below figure, bar = 500 nm. (E) Localization of FOP in the ventral cortex after RNAi, green fluorescence indicates the positive staining for the anti-FOP antibody, and red fluorescence indicates the positive staining for the anti-γ-tubulin antibody, the white triangles indicate the broken off ventral cirri and the black triangle indicates the localization of FOP on the macronucleus, bar = 20 μm. (F) Growth curve of *Euplotes amieti* during RNAi. (G) Relative expression of FOP gene after RNAi, ** $P < 0.01$ *vs* the blank group. (H) Relative expression of FOP protein after RNAi, * $P < 0.01$ *vs* the blank group. Ma, Macronucleus; Mi, Micronucleus; AZM, adoral zone of membranelles; Pm, paroral membrane; FVC, frontoventral cirri; TC, transverse cirri; CC, caudal cirri; LMC, left marginal cirri. PLM, posterior longitudinal microtubules; ALM, anterior longitudinal microtubules.

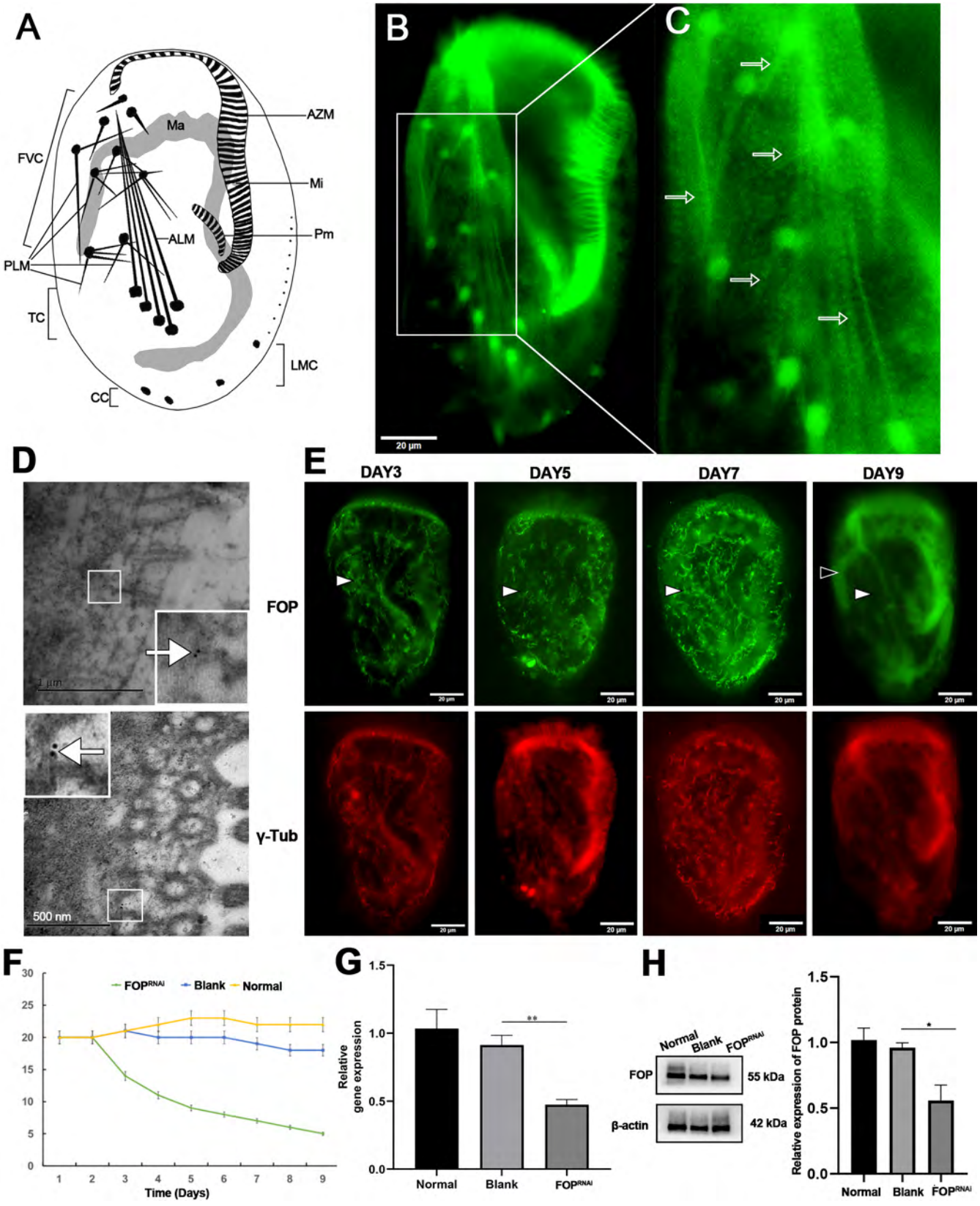
A
AZM
Ma
FVC
Mi
ALM
Pm
PLM
TC
LMC
CC
B
C
20 μm
D
1 μm
500 nm
FOP
γ-Tub
E
DAY3
DAY5
DAY7
DAY9
20 μm
F
FOPRNAi
Blank
Normal
Time (Days)
G
Relative gene expression
Normal
Blank
FOPRNAi
H
Normal
Blank
FOPRNAi
FOP
55 kDa
β-actin
42 kDa
Relative expression of FOP protein

in *Euplotes amieti* following RNAi treatment (Fig. 1E). γ-tubulin was used as a marker of the basal body. The results showed that from the 3rd day, the axoneme of ventral cirri, such as the adoral zone of membranelles, the frontal-ventral-transverse-caudal cirri, and the marginal cirri, gradually broke off from their basal bodies. On the 7th day, most of the ciliary microtubules had disassembled but the basal bodies still existed. On the 9th day, the ventral basal bodies could not be observed except in the adoral zone of the membranelles.

Part of the microtubule structure of *Euplotes amieti* was disassembled after interference

Localization of Flutax-2 was used to show changes in the ciliary basal body and microtubular cytoskeleton in *Euplotes amieti* after RNA interference treatment to suppress the expression of FOP at 3 d, 5 d, 7 d, and 9 d (Fig. 2A).

The results showed that the structure of the cilia and their accessory microtubules in *Euplotes amieti* changed as the number of interference days increased. On the 3rd day after RNA interference, in the interference group, part of the ALM, and the PLM of transverse cirri had been disassembled. The basal bodies were still present. There were slight positive marks in the nucleus. However, during this same time point, the cellular morphology in the blank group remained unchanged, and the microtubule organelles and basal bodies were still observable. From the 5th day to the 7th day, in the interference group, all the ciliary-associated microtubules were disassembled, and a small number of basal bodies of FVC and the membranes of the adoral zone of membranelles were also visible. On the 9th day, almost all of the ciliary microtubules in the *Euplotes amieti* in the interference group were not labeled by Flutax-2. It was hard to observe basal bodies of the ventral cirri, the structure of the adoral zone of membranelles had begun to disintegrate gradually, and the membranes had become thinner. However, the cellular morphology of the Euplotes in the blank group had not changed significantly compared to that observed from the 5th day to the 9th day. In addition, the morphology of the macronucleus didn't change in all the groups during FOP interference (S2A–D).

The cortical microtubule cytoskeleton of *Euplotes amieti* was disassembled after RNAi

As shown by transmission electron microscopy, *Euplotes amieti* has developed dorsal-ventral differentiated structures and forms different cortical microtubules, which are the ciliated microtubules and non-ciliated microtubules. The non-ciliated cortex of Euplotes contains microtubule organelles formed by the polymerization of single or multiple microtubules. Various microtubule organelles are localized in a specific cortex with different structural features.

The dorsal subcortical microtubules in the normal group contained triplet microtubules, which formed a triangle structure, arranged at 30 nm intervals. The same structure was observed in the blank group. In contrast in the interference group, this structure in the dorsal cortex was not present, and they had lost 1–2 triplet microtubules. In addition, the ventral subcortical microtubules were formed by a single microtubule arranged at 70–90 nm intervals in the normal group, however, in the interference group, some subcortical microtubules in the ventral cortex disappeared (Fig. 2B).

The expression of FOP-related proteins decreased following RNAi

The efficiency of the RNAi was validated by assessing the expression of proteins associated with microtubule assembly and basal bodies using western blotting. The results showed there were no significant differences in the expression levels of γ-tubulin between the interference, blank, and normal groups ($P > 0.05$) (Fig. 3C). However, the expression levels of IFT88 and BBS8 were significantly decreased in the interference groups ($p < 0.05$), indicating that these ciliary assembly-associated proteins were downregulated when FOP expression was silenced (Fig. 3A and B). The above results suggest that FOP may be involved in the cilia

➤➤

Figure 2. Changes in the microtubule cytoskeletons of *Euplotes amieti* before and after RNAi. (A) *Euplotes amieti* were labeled with Flutax-2 on the 3rd, 5th, 7th, and 9th days after being fed with *E.coli* HT115. FOP^{RNAi} represents the interference group. Arrows indicate the cilia-associated microtubules, blank triangles indicate the CC and white triangles indicate the FVC. Bar = 20 μm. (B) Ultrastructure of cortical microtubules in *Euplotes amieti* after RNAi. The above figures are from the dorsal cortex, and the below figures are from the ventral cortex. The white triangles indicate the typical triplet microtubules in the dorsal cortex of Euplotes. The black triangles indicate the single microtubule in the ventral cortex of Euplotes. Arrows indicate the microtubule disassembly in the dorsal and ventral cortex after RNAi. Bar = 500 nm.

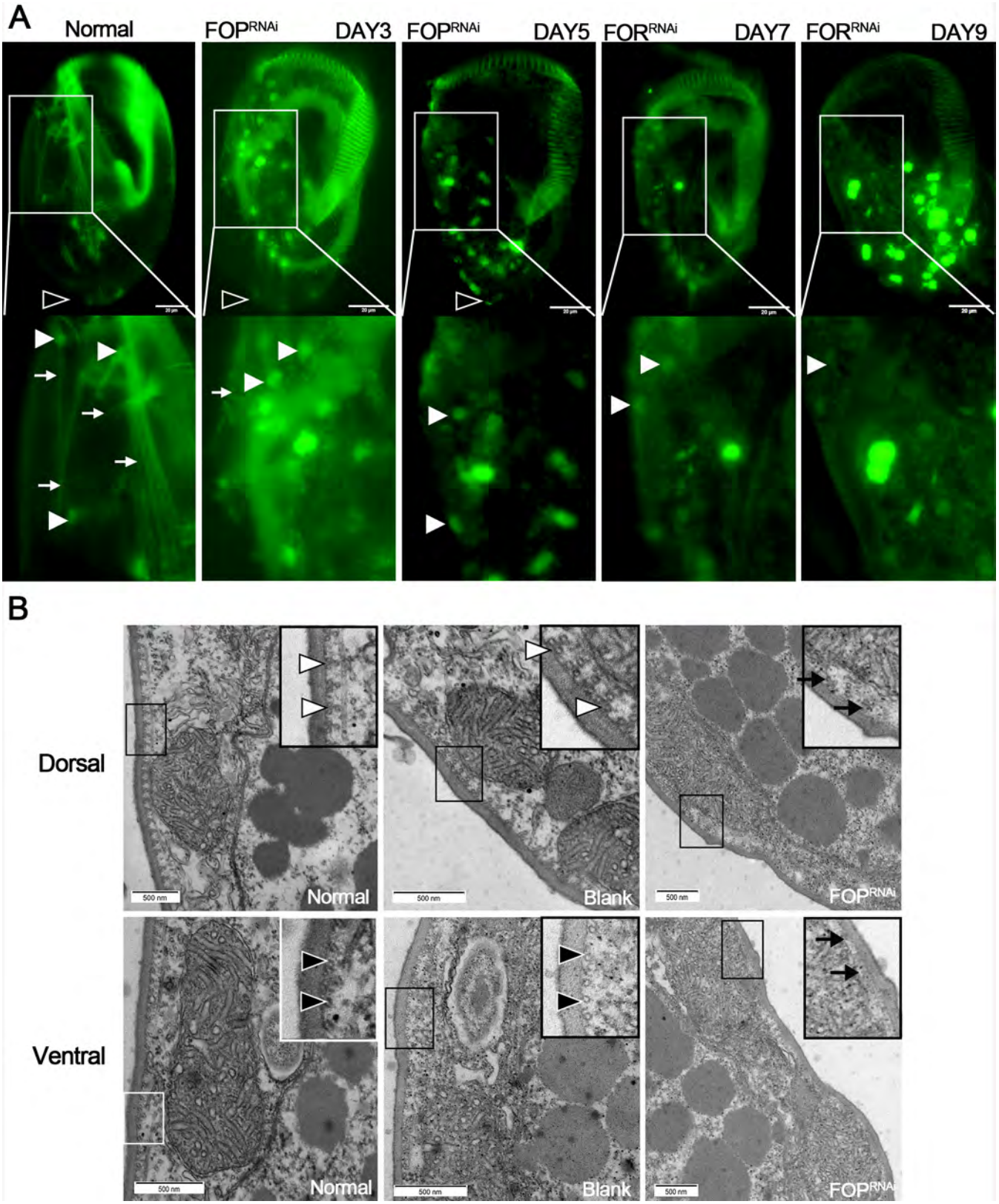
A
Normal
FOPRNAi DAY3
FOPRNAi DAY5
FORRNAi DAY7
FORRNAi DAY9
B
Dorsal
Ventral
Normal
Blank
FOPRNAi
Normal
Blank
FOPRNAi
500 nm

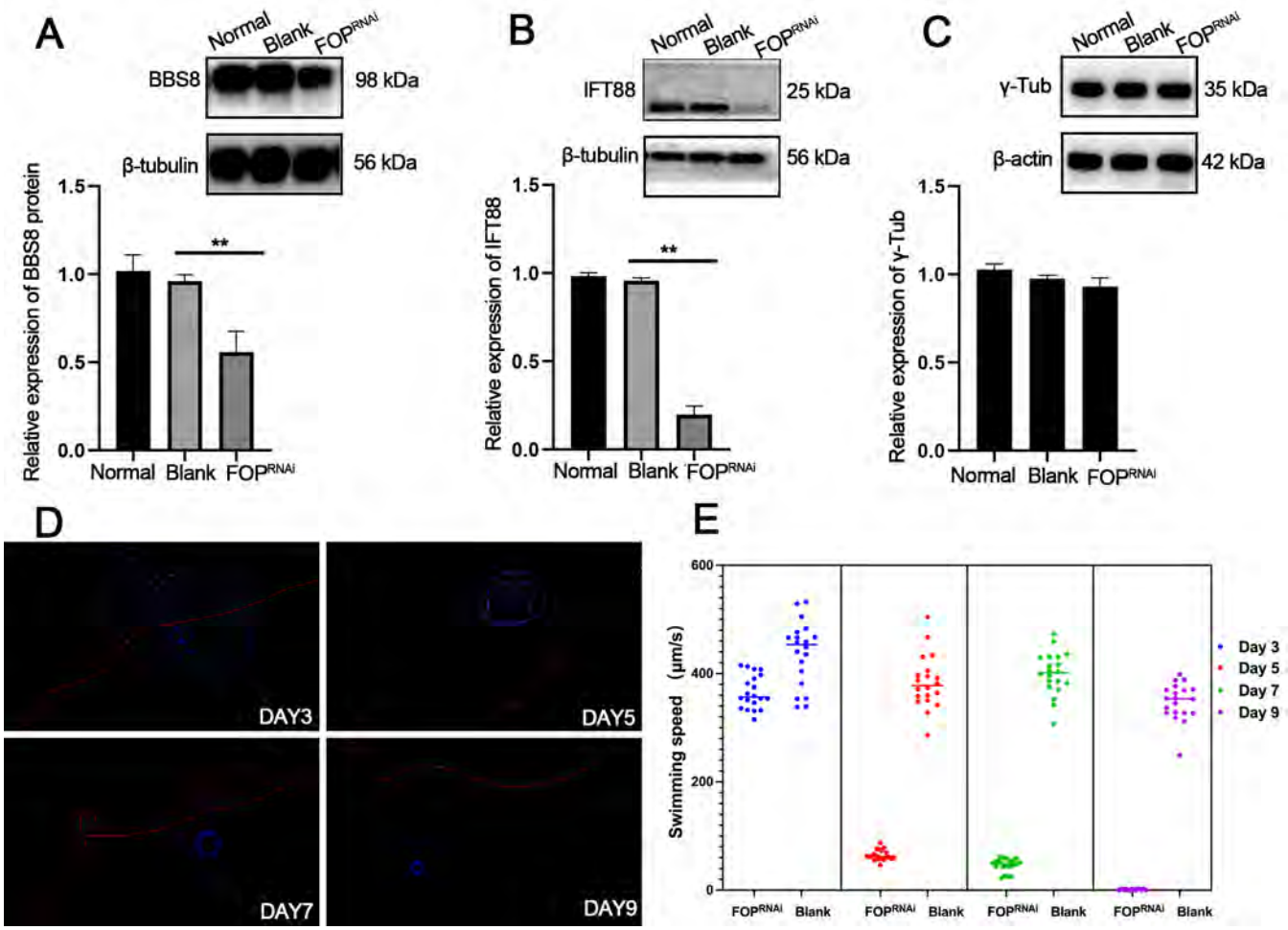

Figure 3. Protein loss and motility changes after RNAi. (A) Relative expression of basal body-associated protein BBS8. $^{**}P < 0.01$ *vs* the blank group, n = 3. (B) Relative expression of cilia assembly-related protein IFT88. $^{**}P < 0.01$ *vs* the blank group, n = 3. (C) Relative expression of basal body protein γ-tubulin. (D) The swimming tracks of *Euplotes amieti* during RNAi. The swimming speeds (n = 20). The FOP^{RNAi} is the interference group, The Blank is the blank group (E) The swimming speeds of *Euplotes amieti* during RNAi (n = 20).

assembly in association with the cilia assembly-related proteins BBS8 and IFT88.

The swimming speed of *Euplotes amieti* decreased and the swimming trace changed after RNAi

We have shown that interfering with FOP expression affected ciliary microtubule stability in *Euplotes amieti*. To detect whether it also affected swimming speeds or trajectories, Gogendeau's (2020) approach was referred to with some improvements. In total, 4–8 *Euplotes amieti* were transferred to a 90 mm Petri dish and covered with slides. Images were captured using a 10× microscope objective every 0.3 sec (Olympus IX83) and analyzed using Prism and ImageJ software.

After RNAi application via feeding, the swimming traces, and velocities of *Euplotes amieti* were measured (Fig. 3D and E). The results showed that, on the 3rd day, cells in the blank group moved along a straight line at a speed of 300–500 μm per second. In contrast, the *Euplotes amieti* in the interference group moved along a curve, and the swimming speed decreased to 300–400 μm per second. On the 5th day after feeding, the swimming traces and speeds of the *Euplotes amieti* in the blank group did not change, whereas the *Euplotes*

amieti in the interference group had lost their ability to swim in a straight line and instead swam in curves/circles. Their swimming speed had also reduced to approximately 40–70 μm per second. On the 7th day of feeding, *Euplotes amieti* in the blank group maintained to swim in a straight line at speeds of 300–400 μm per second. However, the movement track of *Euplotes amieti* in the interference group was still circular, and the swimming speed had decreased even further than observed on the 5th day, down to 30–60 μm per second. On the 9th day, the *Euplotes amieti* silenced with FOP had completely lost the ability to travel in a straight line, moving only on circular paths, and the swimming speed was just 2 μm per second.

DISCUSSION

FOP is an important component of centriole satellites, which are also located in centrosomes. Centrosomal satellites have been extensively studied in drosophila and mammals. They are dense particles composed of many proteins involved in microtubule organization and interact with ciliated proteins (Quarantotti et al. 2019). Our previous work showed that FOP was co-localized with γ-tubulin. In the present study, we found that FOP was mainly located in the basal and basal body microtubules of the ventral cilia in *Euplotes amieti*. No localization was observed in the dorsal microtubule organelles such as the dorsum cirri and the dargyrome, indicating that the protein did not participate in the assembly of the dorsum cirri and the dargyrome. The immunofluorescence results also showed that FOP was located in the accessorial microtubule of ciliary organelles and the basal body. Bornens (2002) demonstrated that the basal body is a very important structure for microtubule anchoring and that the CAP350-FOP complex provides a centrosome docking site for tubulin for microtubule nucleation extension. Interference with FOP expression leads to loss of microtubule anchoring function and severe disruption of the network (Yan et al. 2006). In *Euplotes amieti*, which has well-developed microtubule organelles, similar phenomena were present when FOP expression was silenced. The immunofluorescence results following interference showed that the ventral ciliary axoneme gradually showed different degrees of breakage as RNAi progressed. On the 9th day, FOP was not observed on the ventral surface of *Euplotes amieti*, and the microtubule organelles marked by Flutax-2 were disassembled. In addition, the *Euplotes amieti* in the interference group could not swim in a straight line and gradually lost their swimming ability as time progressed, with a complete loss in swimming ability by day 9 of interference. Early studies have shown that in cilia, the wobble of cilia requires sustained energy flow from the basal body to the front dynein, and loss of function in ciliary genes increases stress cilia formation, impairs ciliogenesis, and decreases swimming speed. As each division of Euplotes is accompanied by cilia depolymerization and reassembly (Ammermann 1971), most of the cilia on the cell surface of *Euplotes amieti* stopped assembly as the number of days of interference increased. The above results suggest that the FOP protein is important and involved in cilium formation, and may regulate assembly of ciliary central microtubule dynein, which regulates the beat of cilia.

Western blotting showed that the expression levels of BBS8 and IFT88 decreased significantly, while that of γ-tubulin remained unchanged in the FOP interference group. These results further indicate that FOP may interact with BBS8, a basal body-associated protein, and acts as a central link between the basal body and axoneme and promotes the cilium assembly protein and transports proteins to the front of the cilia, thus promoting cilia assembly.

FOP has been shown to be a centrosome protein throughout the cell cycle. In ciliates, FOP is also located in the basal bodies, they are microtubule organizing centers during axoneme assembly. It has been reported that excess FOP after cilia assembly is "sequestered" in the G2 phase (Acquaviva et al. 2009), but where the FOP protein is sequestered to is not clearly indicated. In the present study, following FOP protein expression interference, some FOP was present in the nucleus. As a signature protein in the microtubule organizing center, γ-tubulin was first discovered by Stearns et al. (1991), forming centrosomes in vitro in the presence of ATP, which suggested that γ-tubulin can also regulate protein nucleation. Therefore, we hypothesized that the γ-tubulin complex plays a regulatory role in cilia assembly and can recruit redundant FOP to the macronucleus in Euplotes following ciliogenesis. In summary, FOP is involved in the ventral ciliary basal body and the whole process of ciliogenesis in *Euplotes amieti*, and the γ-tubulin complex can regulate FOP after ciliogenesis.

Euplotes amieti have shown special dorsal-ventral differentiation, such as the ventral cirri which assemble into bundles and form different microtubule organelles

that perform different functions. In *Euplotes amieti*, the structure of non-ciliated microtubule organelles is different in the ventral and dorsal cortex. The ventral subcortical microtubule layer is formed by a single microtubule, whereas the dorsal subcortical microtubule layer is formed by a triplet structure (Fleury 1991). Transmission electron microscopy showed that when FOP expression was silenced, the subcortical microtubule structure disappeared completely. Furthermore, as the number of interference days increased, the cortical microtubule gradually depolymerized and the cells became larger. This indicated that FOP participated in the maintenance of the cortical microtubule cytoskeleton on the dorsal and ventral surfaces, and the subcortical microtubules play an important role in maintaining the morphological structure of ciliates.

Acknowledgments. This work was supported by grants from the National Natural Science Foundation of China (NSFC-31760616), and the Science and Technology Foundation of Guizhou Province (Qiankehejichu-ZK [2022] zhongdian 050). Special thanks also to the editors of EditSprings (https://www.editsprings.cn) for the expert linguistic services provided.

REFERENCES

Acquaviva C., Chevrier V., Chauvin J. P., Fournier G., Birnbaum D., Rosnet O. (2009) The centrosomal FOP protein is required for cell cycle progression and survival. *Cell Cycle* **8**: 1217–1227

Ammermann D. (1971) Morphology and development of the macronuclei of the ciliates *Stylonychia mytilus* and *Euplotes aediculatus*. *Chromosoma* **33**: 209–238

Bayless B. A., Galati D. F., Pearson C. G. (2015) Tetrahymena basal bodies. *Cilia* **5**: 1–5

Berbari N. F., Sharma N., Malarkey E. B., Pieczynski J. N., Boddu R., Gaertig J., Guay-Woodford L., Yoder B. K. (2013) Microtubule modifications and stability are altered by cilia perturbation and in cystic kidney disease. *Cytoskeleton* **70**: 24–31

Bornens M. (2002) Centrosome composition and microtubule anchoring mechanisms. *Curr. Opin. Cell Biol.* **14**: 25–34

Bouhouche K., Valentine M. S., Le Borgne P., Lemullois M., Yano J., Lodh S., Nabi A., Tassin A. M., Van Houten J. L. (2022) Paramecium, a model to study ciliary beating and ciliogenesis: Insights from cutting-edge approaches. *Front. Cell Dev. Biol.* **10**: 847908

Cabaud O., Roubin R., Comte A., Bascunana V., Sergé A., Sedjaï F., Birnbaum D., Rosnet O., Acquaviva C. (2018) Mutation of FOP/FGFR1OP in mice recapitulates human short rib-polydactyly ciliopathy. *Hum. Mol. Genet.* **27**: 3377–3391

Chen X., Shi Z., Yang F., Zhou T., Xie S. (2023) Deciphering cilia and ciliopathies using proteomic approaches. *FEBS J.* **290**: 2590–2603

Deane J. A., Cole D. G., Seeley E. S., Diener D. R., Rosenbaum J. L. (2001) Localization of intraflagellar transport protein IFT52 identifies basal body transitional fibers as the docking site for IFT particles. *Curr. Biol.* **11**: 1586–1590

Dentler W. L. (1980) Structures linking the tips of ciliary and flagellar microtubules to the membrane. *J. Cell. Sci.* **42**: 207–220

Fleury A. (1991) Dynamics of the cytoskeleton during morphogenesis in the ciliate Euplotes: II. Cortex and continuous microtubular systems. *Eur. J. Protistol.* **27**: 220–237

Forsythe E., Kenny J., Bacchelli C., Beales P. L. (2018) Managing Bardet – Biedl syndrome – now and in the future. *Front. Pediatr.* **6**: 23

Gherman A., Davis E. E., Katsanis N. (2006) The ciliary proteome database: An integrated community resource for the genetic and functional dissection of cilia. *Nat. Genet.* **38**: 961–962

Goetz S. C., Anderson K. V. (2010) The primary cilium: A signaling centre during vertebrate development. *Nat. Rev. Genet.* **11**: 331–344

Gogendeau D., Lemullois M., Le Borgne P., Castelli M., Aubusson-Fleury A., Arnaiz O., Cohen J., Vesque C., Schneider-Maunoury S., Bouhouche K., Koll F., Tassin, A. M. (2020) MKS-NPHP module proteins control ciliary shedding at the transition zone. *PLOS Biol.* **18**: e3000640

Ishikawa H., Marshall W. F. (2011) Ciliogenesis: Building the cell's antenna. *Nat. Rev. Mol. Cell Bio.* **12**: 222–234

Lee J. Y., Stearns T. (2013) FOP is a centriolar satellite protein involved in ciliogenesis. *PlOS one* **8**: e58589

Libusová L., Dráber P. (2006) Multiple tubulin forms in ciliated protozoan Tetrahymena and Paramecium species. *Protoplasma* **227**: 65–76

Loktev A. V., Zhang Q., Beck J. S., Searby C. C., Scheetz T. E., Bazan J. F., Slusarski D. C., Sheffield V. C., Jackson P. K., Nachury M. V. (2008) A BBSome subunit links ciliogenesis, microtubule stability, and acetylation. *Dev. Cell* **15**: 854–865

Meehl J. B., Bayless B. A., Giddings T. H., Pearson C. G., Winey M. (2016) Tetrahymena Poc1 ensures proper intertriplet microtubule linkages to maintain basal body integrity. *Mol. Bio. Cell* **27**: 2394–2403

Mikolajka A., Yan X., Popowicz G. M., Smialowski P., Nigg E. A., Holak T. A. (2006) Structure of the N-terminal domain of the FOP (FGFR1OP) protein and implications for its dimerization and centrosomal localization. *J. Mol. Biol.* **359**: 863–875

Mockel A., Perdomo Y., Stutzmann F., Letsch J., Marion V., Dollfus H. (2011) Retinal dystrophy in Bardet–Biedl syndrome and related syndromic ciliopathies. *Prog. Retin. Eye Res.* **30**: 258–274

Paschka A. G., Jönsson F., Maier V., Möllenbeck M., Paeschke K., Postberg J., Rupprecht S., Lipps H. J. (2003) The use of RNAi to analyze gene function in spirotrichous ciliates. *Eur. J. Protistol.* **39**: 449–454

Pearson C. G., Winey M. (2009) Basal body assembly in ciliates: The power of numbers. *Traffic* **10**: 461–471

Quarantotti V., Chen J. X., Tischer J., Gonzalez Tejedo C., Papachristou E. K., D'Santos C. S., Kilmartin J. V., Miller M. L., Gergely F. (2019) Centriolar satellites are acentriolar assemblies of centrosomal proteins. *EMBO J.* **38**: e101082

Reiter J. F., Leroux M. R. (2017) Genes and molecular pathways underpinning ciliopathies. *Nat. Rev. Mol. Cell Bio.* **18**: 533–547

Shen C., Gao J., Sheng Y., Dou J., Zhou F., Zheng X., Ko R., Tang X., Zhu C., Yin X., Sun L., Cui Y., Zhang X. (2016) Genetic susceptibility to vitiligo: GWAS approaches for identifying vitiligo susceptibility genes and loci. *Front. Genet.* **7**: 3

Stearns T., Evans L., Kirschner M. (1991) γ-Tubulin is a highly conserved component of the centrosome. *Cell* **65**: 825–836

Vizmanos J. L., Hernández R., Vidal M. J., Larráyoz M. J., Odero M. D., Marín J., Ardanaz M. J., Calasanz M. J., Cross, N. C. (2004) Clinical variability of patients with the t (6; 8)(q27; p12) and FGFR1OP-FGFR1 fusion: Two further cases. *The Hematology*

Journal: The Official Journal of the European Haematology Association **5**: 534–537

Williams C. L., Li C., Kida K., Inglis P. N., Mohan S., Semenec L., Bialas N. J., Stupay R. M., Chen N., Blacque O. E., Yoder B. K., Leroux M. R. (2011) MKS and NPHP modules cooperate to establish basal body/transition zone membrane associations and ciliary gate function during ciliogenesis. *J. Cell Biol.* 192: 1023–1041

Yan X., Habedanck R., Nigg E. A. (2006) A complex of two centrosomal proteins, CAP350 and FOP, cooperates with EB1 in microtubule anchoring. *Mol. Biol. Cell* **17**: 634–64

Received on 3rd August, 2023; revised on 6th November, 2023; accepted on 22nd November 2023

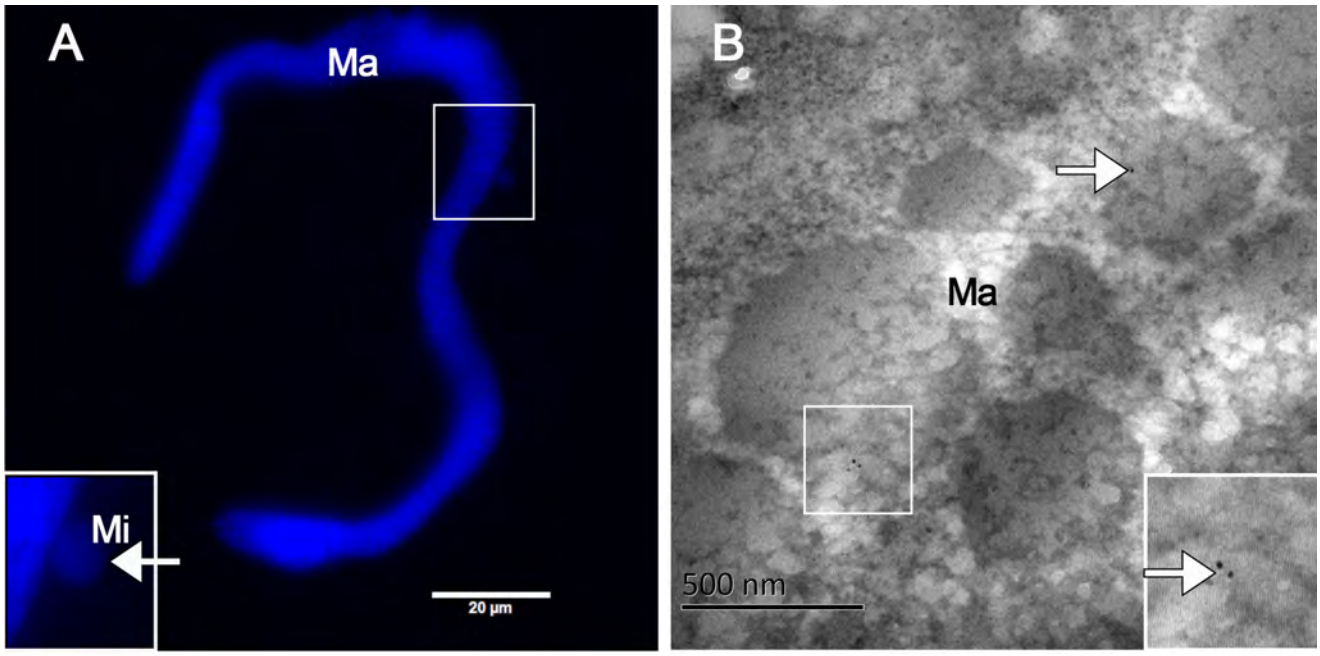

S1. The morphology of the nucleus of *Euplotes amieti* and the localization of FOP. (A) The nucleus of *Euplotes amieti* labeled by DAPI. Arrow indicates the micronucleus. Bar = 20 μm. (B) Localization of FOP protein in the macronucleus of *Euplotes amieti*, arrow indicates the gold particles. Bar = 500 nm.

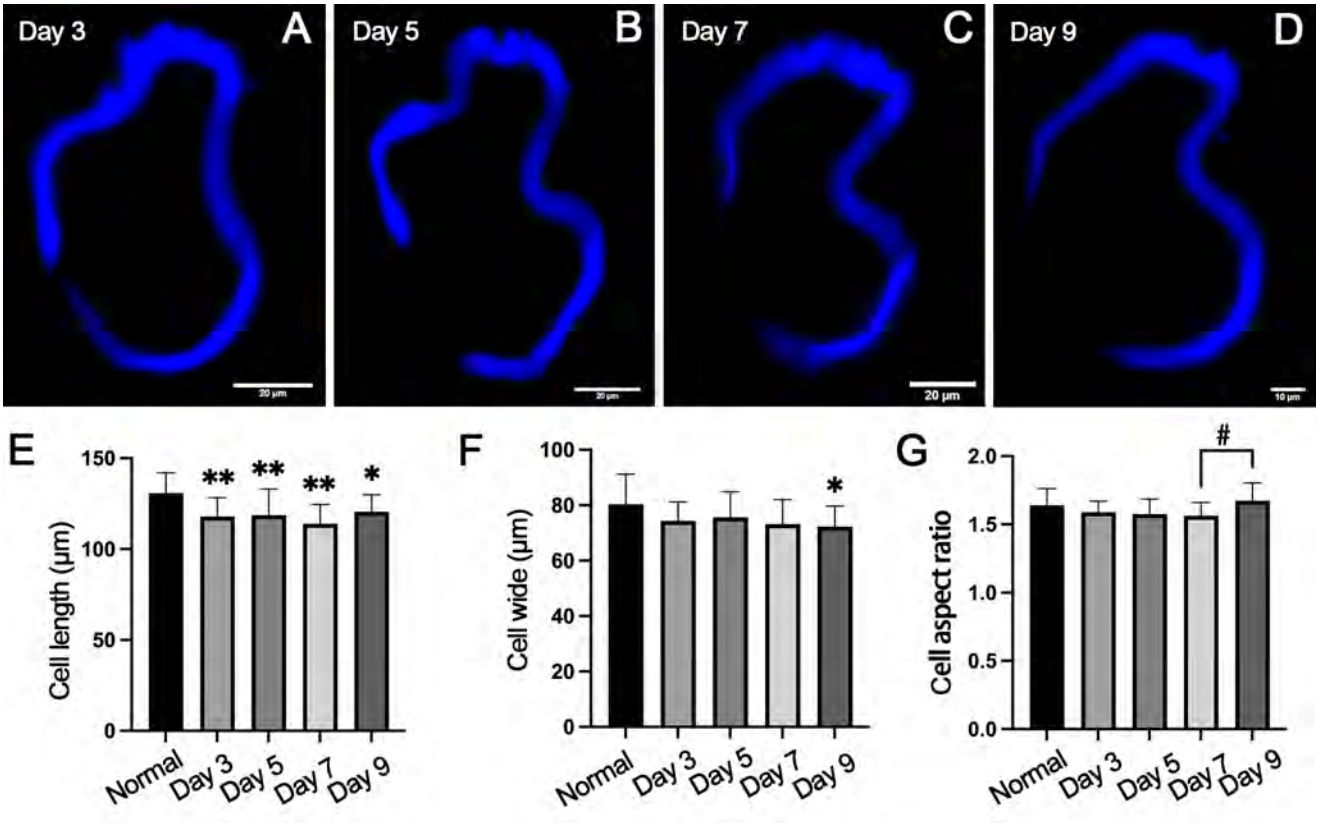

S2. Changes in the morphology of the macronucleus and cell sizes of *Euplotes amieti* after RNAi. (A) The nucleus of *Euplotes amieti* labeled by DAPI after RNAi. Bar = 20 μm. (B) Changes in the cell sizes of *Euplotes amieti*. * $P < 0.05$, **$P < 0.01$ vs the normal group, n = 16; # $P < 0.05$, vs the cells on the 7th day, n = 16